Neutral glycolipids of the filamentous fungus *Neurospora crassa*: altered expression in plant defensin-resistant mutants[S]

Chaeho Park,* Beau Bennion,† Isabelle E. J. A. François,§ Kathelijne K. A. Ferket,§ Bruno P. A. Cammue,§ Karin Thevissen,§ and Steven B. Levery[1,†]

Complex Carbohydrate Research Center and Department of Biochemistry and Molecular Biology,* University of Georgia, Athens, GA 30602-7229; Department of Chemistry,† University of New Hampshire, Durham, NH 03824-3598; and Center of Microbial and Plant Genetics,§ Katholieke Universiteit Leuven, B-3001 Heverlee-Leuven, Belgium

Abstract **To defend themselves against fungal pathogens, plants produce numerous antifungal proteins and peptides, including defensins, some of which have been proposed to interact with fungal cell surface glycosphingolipid components. Although not known as a phytopathogen, the filamentous fungus *Neurospora crassa* possesses numerous genes similar to those required for plant pathogenesis identified in fungal pathogens (Galagan, J. E., et al. 2003. *Nature* 422: 859–868), and it has been used as a model for studying plant-phytopathogen interactions targeting fungal membrane components (Thevissen, K., et al. 2003. *Peptides*. 24: 1705–1712). For this study, neutral glycolipid components were extracted from wild-type and plant defensin-resistant mutant strains of *N. crassa*. The structures of purified components were elucidated by NMR spectroscopy and mass spectrometry. Neutral glycosphingolipids of both wild-type and mutant strains were characterized as β-glucopyranosylceramides, but those of the mutants were found with structurally altered ceramides. Although the wild type expressed a preponderance of *N*-2′-hydroxy-(*E*)-Δ^3-octadecenoate as the fatty-*N*-acyl component attached to the long-chain base (4*E*,8*E*)-9-methyl-4,8-sphingadienine, the mutant ceramides were found with mainly *N*-2′-hydroxyhexadecanoate instead. In addition, the mutant strains expressed highly increased levels of a sterol glucoside identified as ergosterol-β-glucoside.[JLR] The potential implications of these findings with respect to defensin resistance in the *N. crassa* mutants are discussed.**—Park, C., B. Bennion, I. E. J. A. François, K. K. A. Ferket, B. P. A. Cammue, K. Thevissen, and S. B. Levery. **Neutral glycolipids of the filamentous fungus *Neurospora crassa*: altered expression in plant defensin-resistant mutants. *J. Lipid Res.* 2005. 46: 759–768.**

Supplementary key words ergosterol • sphingolipid • sterol • glucoside • ceramide • cerebroside • electrospray ionization • nuclear magnetic resonance spectroscopy • mass spectrometry • collision-induced dissociation • tandem mass spectrometry

Manuscript received 17 November 2004 and in revised form 14 January 2005.

Published, JLR Papers in Press, January 16, 2005.
DOI 10.1194/jlr.M400457-JLR200

Plants possess an impressive arsenal of antimicrobial compounds that are either constitutively arrayed within certain tissues or synthesized in direct response to attack by pathogens. Among these compounds are defensins, a class of evolutionarily and structurally related small, highly basic, cysteine-rich peptides, many of which display antifungal activity (reviewed in 1–3). Defensins are also found in other types of organisms, including insects and humans, as important components of innate immunity (4–6). The structures of human, insect, and plant defensins, which include a conserved amphipathic β-sheet motif, are consistent with a membranolytic mode of action, but plant defensins, unlike those of humans and insects, have not been shown to induce ion-permeable pores in artificial membranes composed of phospholipids or to change the electrical properties of artificial lipid bilayers (3). Nevertheless, some plant defensins have been shown to induce rapid increases in potassium efflux and calcium uptake in *Neurospora crassa* hyphae (7), and plant defensin-induced membrane permeabilization of *N. crassa* and *Saccharomyces cerevisiae* cells, as measured by SYTOX green uptake, was correlated with the inhibition of growth (8). In addition, using the *N. crassa* and *S. cerevisiae* model systems, high-affinity binding of plant defensins to fungal cells and membrane fractions has been demonstrated and also correlated with their antifungal activity (9, 10).

Recent investigations have implicated sphingolipids as targets of defensin binding to the fungal membrane (11–

Abbreviations: CID, collision-induced dissociation; ESI, electrospray ionization; Fa, fatty acyl; GlcCer, β-glucopyranosylceramide; GlcSte, steryl-β-glucopyranoside; HPTLC, high-performance thin-layer chromatography; TOF, time-of-flight; UGT, UDP-Glc:sterol β-D-glucosyltransferase.

[1] To whom correspondence should be addressed.
e-mail: slevery@cisunix.unh.edu

[S] The online version of this article (available at http://www.jlr.org) contains an additional figure and table.

13). The sensitivity of *S. cerevisiae* to DmAMP1, a defensin isolated from the seeds of *Dahlia merckii* (14), was shown to be dependent on *IPT1* (15), a gene required for the final step in the biosynthesis of the complex yeast sphingolipid mannose-(inositol-phosphate)$_2$-ceramide (16). Moreover, using an ELISA, DmAMP1 was found to interact in a dose-dependent manner with *S. cerevisiae* sphingolipids, and this interaction was enhanced in the presence of ergosterol, the major sterol component of fungi (12). More recently, the sensitivity of the yeasts *Pichia pastoris* and *Candida albicans* toward RsAFP2, a defensin isolated from seeds of *Raphanus sativus* (radish) (17), was found to be dependent on *GCS* (13), the gene encoding glucosylceramide synthase (UDP-Glc:ceramide β-glucosyltransferase) (18). In that study, interaction of RsAFP2 was observed with β-glucopyranosylceramide (GlcCer) isolated from *P. pastoris* but not from soybean or human (13), which differ in the structures of their ceramide moieties. Finally, chemically mutagenized *N. crassa* strains selected for resistance to RsAFP2 were found to have dramatically altered glycolipid/sphingolipid expression profiles (11). Although a number of these differences are obvious from even superficial glycolipid profiling by thin-layer chromatography, as described previously (11), the true nature of some alterations, particularly with respect to neutral glycolipid expression, required detailed structural analysis to become apparent. The structural characterization of these neutral glycolipid components, isolated from wild-type and defensin-resistant mutant *N. crassa* strains, is described in this report.

MATERIALS AND METHODS

Fungal isolate and growth conditions

N. crassa [(strain 74-OR23-1A; Fungal Genetics Stock Center (FGSC) number 987, American Type Culture Collection number 24698; termed wild type (WT)] and its mutants were grown on half-strength potato dextrose broth agar (12 g/l potato dextrose broth, 15 g/l agar; Difco, Detroit, MI). For the purposes of lipid extraction, cultures of *N. crassa* WT, MUT16, and MUT24, grown on solid yeast peptone dextrose agar plates at room temperature, were transferred to 1.2 g/l liquid potato dextrose broth medium in 2.5 liter Fernbach flasks and shaken for 3 days at 25°C or 37°C at 250 rpm. Mycelia were harvested by filtration through cheesecloth, washing off excess media with water. Excess water was removed by gentle pressure, and mycelia were either stored at −80°C until extraction or processed immediately as described below.

Solvents for extraction, anion-exchange chromatography, and high-performance thin-layer chromatography

Solvent A is chloroform-methanol (1:1, v/v); solvent B is isopropanol-hexane-water (55:25:20, v/v/v; upper phase discarded). Solvent C consists of chloroform-methanol-water (30:60:8, v/v/v), and solvent D consists of isopropanol-hexane-water (55:40:5, v/v/v). Solvent E is chloroform-methanol-2 N ammonium hydroxide (40:10:1, v/v/v); solvent F is chloroform-methanol-water [50:47:14, v/v/v; containing 0.035% (w/v) $CaCl_2$].

Extraction and purification of glycosphingolipids

Extraction and purification of glycosphingolipids were carried out as described previously (19–21). Briefly, glycosphingolipids were extracted by homogenizing mycelia (40–80 g wet weight) in a glass-walled blender once with 200 ml of solvent A, two times with 200 ml of solvent B, and once more with 200 ml of solvent A. The four extracts were pooled, dried on a rotary evaporator, dialyzed against water, lyophilized, resuspended in solvent C, and applied to a column of DEAE-Sephadex A-25 (Ac^- form). Neutral glycosphingolipids were eluted with five volumes of solvent C. The neutral fraction was then dried and taken up in solvent D before analytical or preparative high-performance thin-layer chromatography (HPTLC) as described below. Acidic glycosphingolipids were eluted with five volumes of 0.5 M sodium acetate in methanol. The acidic fraction was dried, dialyzed exhaustively against deionized water, and redried. Analyis of acidic components will be described elsewhere.

HPTLC

Both analytical and preparative HPTLC were performed on silica gel 60 plates (E. Merck, Darmstadt, Germany) using chloroform-methanol-water [60:40:9, v/v/v; containing 0.02% (w/v) $CaCl_2$ (solvent D)] as mobile phase. Lipid samples were dissolved in solvent B and applied by streaking from 5 μl Micro-caps (Drummond, Broomall, PA). For analytical HPTLC, detection was performed with Bial's orcinol reagent [0.55% (w/v) orcinol and 5.5% (v/v) H_2SO_4 in ethanol-water 9:1 (v/v); the plate is sprayed and heated briefly to ~200–250°C; violet staining is positive for the presence of hexose]. For preparative HPTLC, samples were streaked lengthwise on 10 × 20 cm plates, and separated glycosphingolipid bands were visualized under ultraviolet

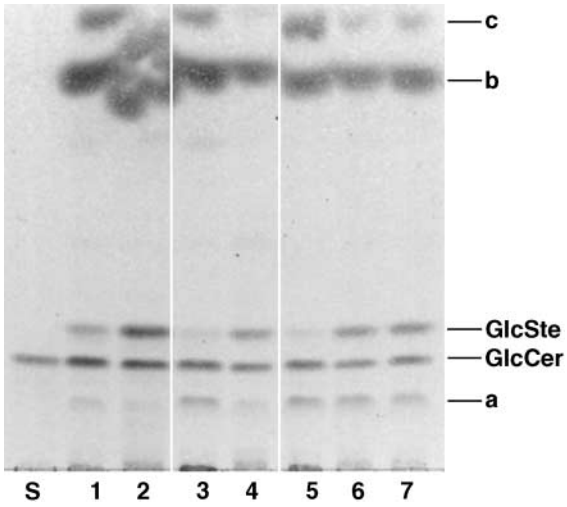

Fig. 1. High-performance thin-layer chromatography profiles of neutral glycolipids from *N. crassa* wild-type (WT), MUT16, and MUT24. Crude neutral lipid fractions, containing steryl-β-glucopyranoside (GlcSte) and β-glucopyranosylceramide (GlcCer), were developed with solvent E; hexose-containing bands were visualized with Bial's orcinol reagent (all bands on the lower section of the gel stained violet, that is, positive for hexose content; bands on the upper section of the gel stained brown to brownish green, that is, negative for hexose content). Lane S, authentic GlcCer from *Aspergillus nidulans* (21); lanes 1, 3, 5, WT; lanes 2, 4, 6, MUT16; lane 7, MUT24. Lanes 1 and 2, 3 and 4, and 5 to 7 [the third set was adapted from the results of Ferket et al. (11)] show lipids extracted from three different sets of cultures that were cultured 2–5 weeks apart. The first and third sets were cultured at 25°C, and the second set was cultured at 37°C; in the second and third sets, samples applied to the gel were diluted in two times the volume of solvent used in the first set. The identities of components a, b, and c have not been unequivocally established.

light after spraying with primulin (Aldrich; 0.01% in 80% aqueous acetone). Bands were marked by pencil and individually scraped from the plate. Glycosphingolipids were then isolated from the silica gel by repeated sonication in solvent A followed by centrifugation. After concentration of the extract, primulin was removed by passage through a short column of DEAE-Sephadex A-25 in solvent C.

^{1}H-nuclear magnetic resonance spectroscopy

Samples of underivatized lipids (~0.5−1.0 mg) were deuterium-exchanged by repeated evaporation from $CDCl_3/CD_3OD$ (2:1, v/v) under an N_2 stream at 35–40°C and then dissolved in 0.5 ml of DMSO-d_6/2% D_2O (22–24) for NMR analysis. One-dimensional ^{1}H-NMR spectra, two-dimensional ^{1}H-^{1}H-gradient-enhanced correlation spectra and total correlation spectra, and two-dimensional ^{1}H-detected ^{1}H-^{13}C-gradient-enhanced heteronuclear single-quantum correlation spectra were acquired at 35°C on Varian Unity Inova 500 MHz (University of New Hampshire, Durham) or 600 or 800 MHz (University of Georgia/Complex Carbohydrate Research Center, Athens) spectrometers using standard acquisition software available in the Varian VNMR software package. Proton chemical shifts are referenced to inter-

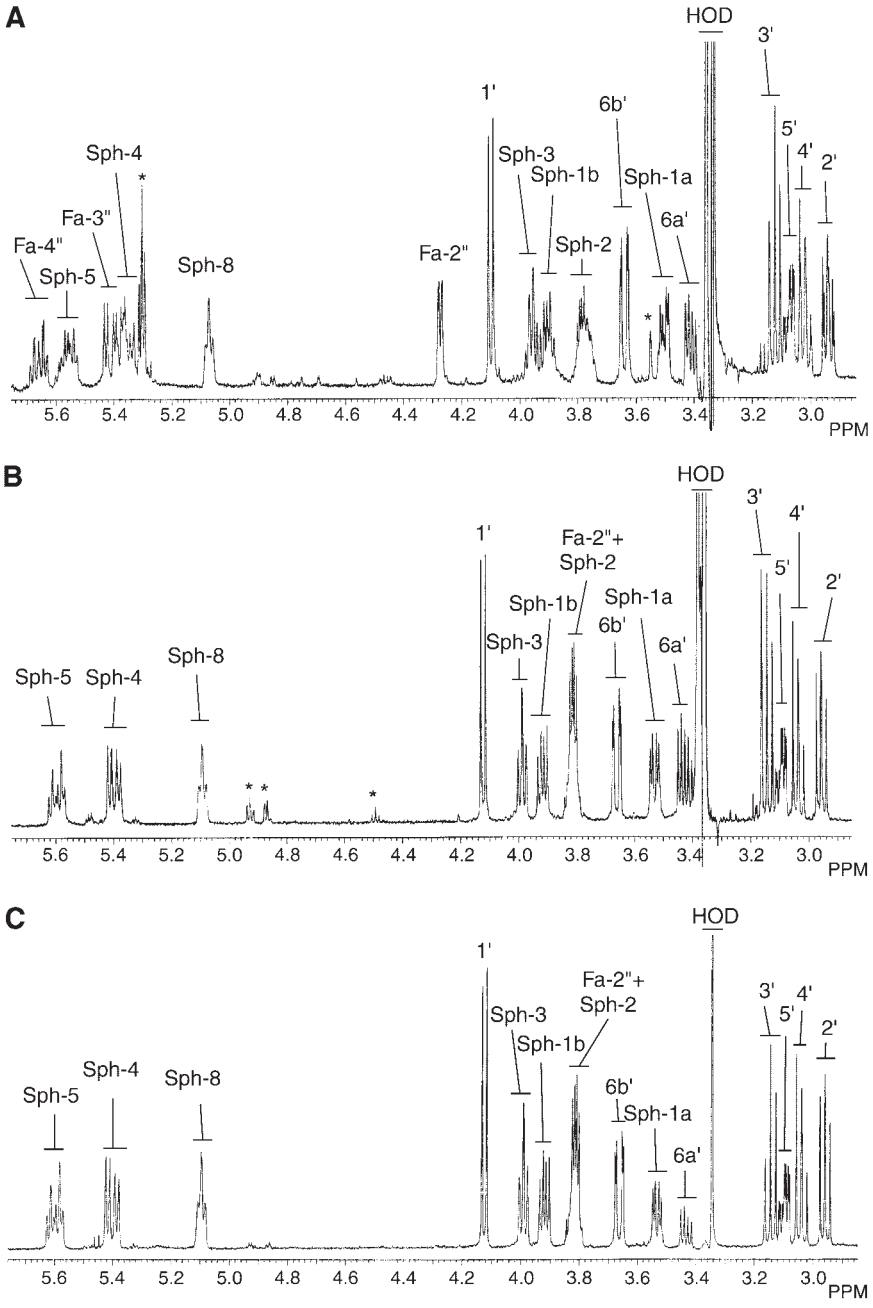

Fig. 2. Downfield sections of one-dimensional ^{1}H-NMR spectra of GlcCer fractions isolated from *N. crassa* strains. A: WT. B: MUT16. C: MUT24. Resonances from nonexchangeable protons of sphingosine (Sph), fatty acyl (Fa), and hexose (prefix omitted) are designated by Arabic numerals (corresponding to those in Scheme 1). Resonances marked by asterisks are from unknown impurities. Fa-2″+ is H-2″ from saturated 2″-hydroxy fatty acid, isochronous with the Sph-2 resonance. HOD, residual monodeuterated water.

nal tetramethylsilane (δ = 0.000 ppm), carbon chemical shifts to the natural abundance ^{13}C-methyl resonance of solvent DMSO-d_6 (δ = 40.00 ppm).

Positive ion mode electrospray ionization mass spectrometry

Mass spectrometry was performed in the positive ion mode on a Micromass (Manchester, UK) hybrid electrospray ionization-Qq/oa-time-of-flight (ESI-Q-TOF)-MS instrument, with sample introduction via direct infusion in 100% methanol (~100 ng/μl; flow rate, 0.5 μl/min). As described previously (25, 26), to generate $[M+Li]^+$ adducts of GlcCer molecular species, LiI (10 mM) in methanol was added to the analyte solution until the observed ratio of $[M+Li]^+$ adducts to mixed Na^+/Li^+ adducts in MS profile mode was >5:1; the necessary LiI concentration was generally in the range 2–3 mM. Resolution was generally 4,000 (5% valley) for positive ion mode ESI ($^+$ESI)-Q-TOF-MS molecular adduct profile spectra and 3,000 for MS/collision-induced dissociation (CID)-TOF-MS experiments. Extraction cone voltage (analogous to orifice-to-skimmer potential in Sciex API series instruments) was 35 V for MS profile spectra and MS/CID-MS experiments. Nominal monoisotopic *m/z* values are used in the labeling and description of $^+$ESI-MS results. Interpretation of spectra derived from $[M+Li]^+$ adducts of GlcCer molecular species was essentially as described previously (25–27).

RESULTS

Detection and isolation of glycolipids from WT and mutant strains of *N. crassa*

Glucosylceramides were initially detected in all of the neutral lipid fractions from *N. crassa* strains, recognized in HPTLC analysis by their orcinol staining and comigration with an authentic standard (11) (**Fig. 1**). There did not appear to be any striking quantitative differences between the WT and mutant strains. In addition, a second orcinol-positive band with relative migration (Rf) higher than GlcCer was detectable in both mutants; this band was also detected in the WT, albeit at significantly lower intensity. It was tentatively proposed to be a sterol glycoside (11), based on its orcinol staining and Rf, compared with recent literature (28, 29). No significant dependence of band intensity on culture temperature (25°C versus 37°C) was apparent for either of the putative glycolipids. Both putative glycolipid components were isolated from the crude neutral lipid fractions of each *N. crassa* strain by preparative HPTLC and characterized by ^{1}H-NMR spectroscopy and ESI-MS. Interestingly, a non-hexose-containing lipid migrating near the solvent front (Fig. 1, band c, staining brown with orcinol) appeared to have a reciprocal quantitative relationship with the putative sterol glycoside band; although its behavior did not appear to be typical of a free sterol or *O*-acyl-sterol, it was also isolated and examined for any potential structural or biosynthetic relationship to the glycosidic components of interest. As this did not appear to be the case (data not shown), its analysis was not pursued further in this study. For similar reasons, detailed analysis of a second component staining brown with orcinol (band b), which appeared in all three strains, was not carried out. An orcinol-positive band with lower Rf (band a) was also detected in all three strains but did not stain with primulin, which detects lipids. ^{1}H-NMR spectroscopy confirmed the absence of resonances characteristic for a lipid component (data not shown).

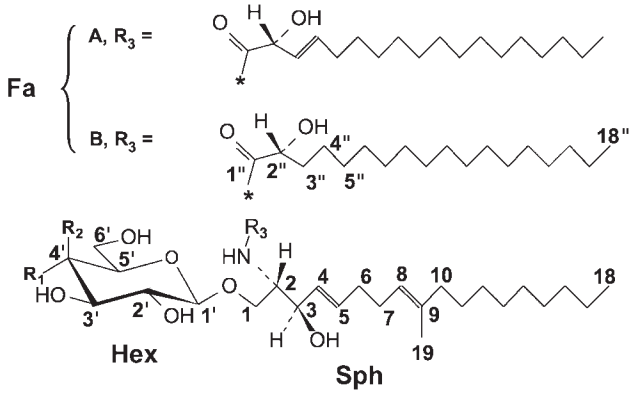

Scheme 1. Structures of prototypical fungal cerebrosides with numbering of sphingosine (Sph), hexose (Hex), and fatty acyl (Fa) moieties: (4*E*,8*E*)-*N*-2″-hydroxyoctadec-(*E*)-3″-enoyl-1-β-D-glucopyranosyl-9-methyl-4,8-sphingadienine (fatty acid R_3 = **A**, R_1 = OH, R_2 = H); (4*E*,8*E*)-*N*-2″-hydroxyoctadec-(*E*)-3″-enoyl-1-β-D-galactopyranosyl-9-methyl-4,8-sphingadienine (fatty acid R_3 = **A**, R_1 = H, R_2 = OH); (4*E*,8*E*)-*N*-2″-hydroxyoctadecanoyl-1-β-D-glucopyranosyl-9-methyl-4,8-sphingadienine (fatty acid R_3 = **B**, R_1 = OH, R_2 = H); and (4*E*,8*E*)-*N*-2″-hydroxyoctadecanoyl-1-β-D-galactopyranosyl-9-methyl-4,8-sphingadienine (fatty acid R_3 = **B**, R_1 = H, R_2 = OH).

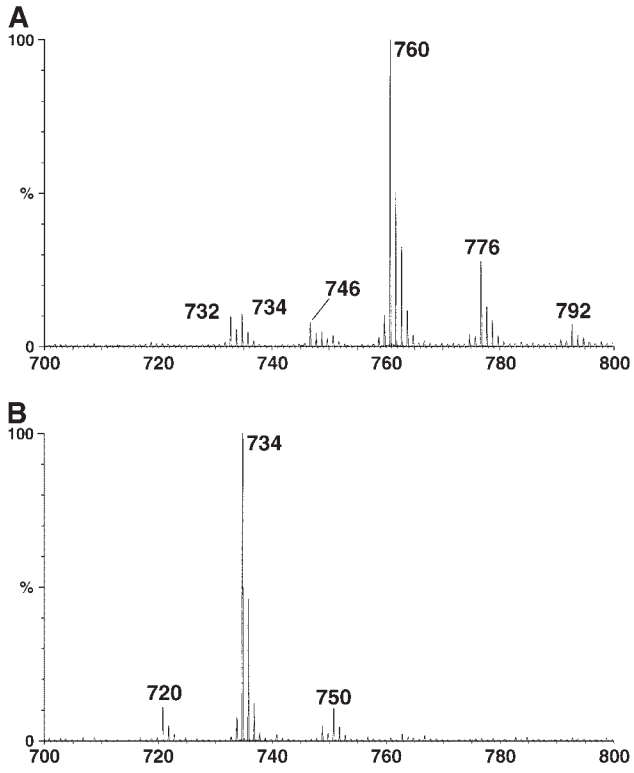

Fig. 3. Lithium molecular adduct profiles from positive ion mode electrospray ionization ($^+$ESI) mass spectrometry of GlcCer fractions isolated from *N. crassa* strains. A: WT. B: MUT16. Peak labels are nominal, monoisotopic *m/z*.

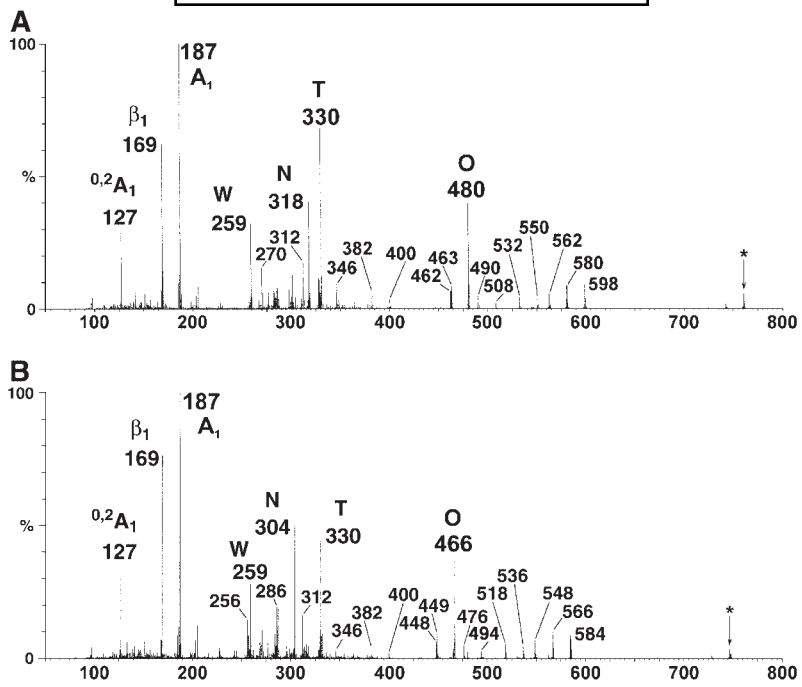

Fig. 4. Tandem $^{+}$ESI-MS/collision-induced dissociation (CID)-MS product ion spectra of selected $[M+Li]^{+}$ from a *N. crassa* WT GlcCer fraction. A: Product ion spectrum from *m/z* 760. B: Product ion spectrum from *m/z* 746.

^{1}H-NMR spectroscopic analysis of *N. crassa* glucosylceramides

Both ^{1}H- and ^{13}C-NMR spectra for several fungal cerebrosides have been previously acquired in DMSO-d_6/2% D_2O at 35°C and all resonances assigned by homonuclear and heteronuclear two-dimensional correlation methods (20, 26). Therefore, it was sufficient for the present work to obtain one-dimensional ^{1}H-NMR spectra from the putative GlcCer components, isolated by preparative HPTLC from each of the three *N. crassa* strains (WT, MUT16, MUT24), to characterize them with respect to monosaccharide identity and key ceramide structural features.

The ^{1}H-NMR spectra confirmed the identity of all three putative GlcCer components (**Fig. 2**; panels A, B, and C correspond to bands marked GlcCer in Fig. 1, lanes 5, 6, and 7, respectively). Each exhibited a set of resonances with chemical shifts and coupling patterns characteristic of the seven proton β-glucopyranosyl spin system (see **Scheme 1** for structures and numbering). Additional resonances in each spectrum identified (4*E*,8*E*)-9-methyl-4,8-sphingadienine along with *N*-2″-hydroxy-(*E*)-3″-alkenoate and/or *N*-2″-hydroxyalkanoate. Interestingly, however, the WT and mutant GlcCer clearly differ with respect to unsaturation of the fatty-*N*-acyl moiety. Key resonances for this feature are those from fatty acyl-3″ (Fa-3″) and Fa-4″, which generally appear at ~5.42–5.44 and 5.66–5.68 ppm, respectively, and from Fa-2″, which is shifted significantly downfield to ~4.28–4.30 ppm, where the unsaturation is present; these signals are clearly visible in the WT GlcCer spectrum (Fig. 2A) but absent in those of the mutants (Fig. 2B, C). Thus,

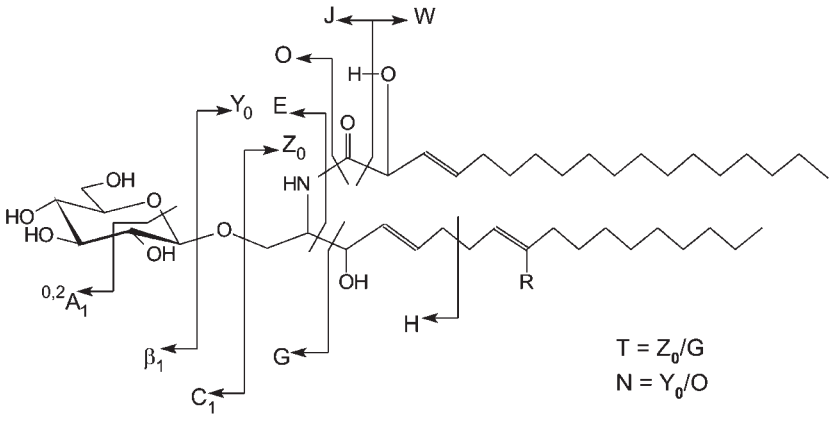

Scheme 2. Fragmentation of a cerebroside with nomenclature of Costello et al. (40–42) as modified by Adams and Ann (43).

although the WT GlcCer exhibits a high level of (*E*)-Δ^3-unsaturation, which can be estimated from the relative integrals of the Fa-4″ and sphingosine-5 resonances, this structural modification appears to be completely ablated in the corresponding mutant fractions.

Note that two resonances are observed at slightly different chemical shifts for the β-Glc H-2′ in the WT GlcCer spectrum, as a result of the long-range influence of the (*E*)-Δ^3-unsaturation in ~70% of the ceramide. An additional key upfield resonance for these compounds is that of the sphingadienine 9-methyl group, which was observed in all three spectra as a singlet at 1.545 ± 0.002 ppm (data not shown). Remaining glycosphingolipid structural features, not conveniently assessed by NMR analysis, are the chain lengths of the Fa and sphingosine moieties. These were determined unambiguously by mass spectrometric methods, which in addition provided confirmation of most of the features discussed above.

Characterization of *N. crassa* glucosylceramides by ESI-MS and tandem MS

In $^+$ESI-Q-TOF-MS, lithiated molecular ions were observed primarily at *m/z* 760 for the WT GlcCer (**Fig. 3A**), consistent with a monohexosylceramide containing (4*E*,8*E*)-9-methyl-4,8-sphingadienine attached to *N*-2″-hydroxy-(*E*)-3″-octadecenoate. In some fractions (data not shown), ion abundance at *m/z* 762 was clearly observed above the theoretical level of the $^{13}C_2$ isotope peak for the major species, consistent with the additional presence of a minor GlcCer component containing saturated *N*-2″-hydroxyoctadecanoate, as noted in the ^{1}H-NMR spectra. Minor components were also observed at *m/z* 746, 734, and 732 (the ion at *m/z* 776 primarily representing residual Na^+ adduct). Details about the ceramide structure of the major and minor components were provided by tandem ESI-MS/CID-TOF-MS experiments (**Fig. 4**). As found previously with MS/CID-MS spectra acquired on a triple quadrupole instrument (25, 26), key ions diagnostic for fatty-*N*-acyl and sphingoid carbon number and level of unsaturation can be observed at high abundance in the hybrid Q-TOF spectra, but with the expected increases in overall sensitivity, resolution, and mass accuracy. In the CID spectrum of the major $[M+Li]^+$ at *m/z* 760, an O ion, corresponding to loss of the fatty-*N*-acyl chain (**Scheme 2**), is observed abundantly at *m/z* 480, characteristic for a monohexosyl-(4*E*,8*E*)-9-methyl-4,8-sphingadienine (25). Additional loss of the hexose moiety yields a confirming N ion, appearing in this spectrum at *m/z* 318. A T ion, derived from loss of the hexose and most of the sphingoid, is observed abundantly at *m/z* 330, providing complementary information about the carbon number and the level of unsaturation of the fatty-*N*-acyl chain, in this case *N*-2″-hydroxy-(*E*)-3″-octadecenoate. This is confirmed by the appearance of a corresponding W ion, particularly characteristic for 2-hydroxy-fatty-*N*-acylation and composed of the acyl C_2-C_ω in the form of an aldehyde, at *m/z* 259. Assignments for other product ions are listed in **Table 1**.

Tandem CID product spectra of minor GlcCer components were also obtainable, enabling in most cases characterization of minor structural variations responsible for the decrements in their molecular masses. For example, in the CID spectrum of the minor $[M+Li]^+$ at *m/z* 746 (Fig. 4B), 14 u decrements are observed almost exclusively for the O and N ions (*m/z* 466 and 304, respectively) but not for the T and W ions, consistent with lack of the branching methyl group on the sphingoid but not with h17:1 fatty-*N*-acylation [this is not always the case (25, 26)]. On the other hand, in the CID spectrum of $[M+Li]^+$ at *m/z* 732 (Table 1), O and N ions are again observed at *m/z* 480 and 318, respectively, but the T and W ions are decremented to *m/z* 302 and 231, respectively, consistent with h16:1 fatty-*N*-acylation. In the CID spectrum of $[M+Li]^+$ at *m/z* 734 (Table 1), the T and W ions are observed at *m/z* 304 and 233, respectively, consistent with saturation of the shorter chain fatty-*N*-acyl moiety (h16:0).

Significantly, in the $^+$ESI-Q-TOF-MS profile of GlcCer from MUT16 (Fig. 3B), the major $[M+Li]^+$ was observed at

TABLE 1. Positive ion mode electrospray ionization-mass spectrometry/collision-induced dissociation-mass spectrometry data (all fragments $\bullet Li^+$ except where noted) for *N. crassa* wild-type β-glucopyranosylceramide (major component, Nc1; minor components, Nc3, Nc4, and Nc5) and mutant β-glucopyranosylceramide (major component, Nc4; minor components, Nc2 and Nc6), with proposed interpretations of fragments

	Wild Type				Mutant		
	Major	Minor			Major	Minor	
	Nc1	Nc3	Nc4	Nc5	Nc4	Nc2	Nc6
Fatty acid	h18:1	h18:1	h16:0	h16:1	h16:0	h18:0	h16:0
Sphingosine	d19:2	d18:2	d19:2	d19:2	d19:2	d18:2	d18:2
M	760	746	734	732	734	748	720
Y_0	598	584	572	570	572	586	558
Z_0	580	566	554	552	554	568	540
H′ (≡ H−H_2O)	562	562	536	534	536	564	536
Z_0−H_2O (≡ Z_0′ ≡ b_2)	562	548	536	534	536	564	522
Z_0−CH_2O (≡a_2)	550	536	524	522	524	538	510
Z_0−CH_2O−H_2O	532	518	—	504	—	—	—
J (≡ M−acyl C_2-C_ω)	508	494	508	508	508	494	496
J′ (≡ J−H_2O)	490	476	490	490	490	476	478
O (≡ M−acyl)	**480**	**466**	**480**	**480**	**480**	**466**	**466**
O′a (≡ M−acyl −NH_3)	463	449	463	463	463	449	449
O′ (≡ M−acyl −H_2O)	462	448	462	462	462	448	448
Z_0/H	400	400	374	372	374	402	—
Z_0/H′ (≡ Z_0/H−H_2O)	382	382	356	354	356	384	—
Z_0/H″ (≡ Z_0/H−2H_2O)	364	364	338	336	338	—	—
S (≡ Y_0/G)	346	346	320	318	320	348	348
T (≡ Z_0/G)	**330**	**330**	**304**	**302**	**304**	**332**	**304**
N (≡ Y_0/O)	**318**	**304**	**318**	**318**	**318**	**304**	**304**
T′ (≡ T−H_2O)	312	312	286	284	286	314	314
U (≡ T−C_2H_2)	304	304	278	278	278	306	306
N′	300	286	300	300	300	286	286
d_{3b}	285	271	285	285	285	271	271
N″ [Li^+]	282	268	282	282	282	268	270
N′−CH_2O (≡ e_{3b})	270	256	270	270	270	256	256
W (acyl C_2-C_ω)	**259**	**259**	**233**	**231**	**233**	**261**	**233**
E	227	227	227	227	227	227	227
C_1	**187**	**187**	**187**	**187**	**187**	**187**	**187**
β_1	**169**	**169**	**169**	**169**	**169**	**169**	**169**
$^{0,2}A_1$	127	127	127	127	127	127	127
$^{0,2}A_1$−CH_2O	97	97	97	97	97	97	97

All values are nominal, monoisotopic *m/z*. Fragment nomenclature is after Costello et al. (40–42) as modified and expanded by Adams and Ann (43) (see **Scheme 3**), with additional designations given by Hsu and Turk (27). The six to seven most abundant fragments in each spectrum are shown in boldface.

m/z 734, consistent with *N*-2″-hydroxyhexadecanoyl-(4*E*,8*E*)-9-methyl-4,8-sphingadienine as the most abundant ceramide component. This ceramide composition was confirmed by acquisition of a tandem CID spectrum (**Fig. 5A**), which exhibited O and N product ions at *m/z* 480 and 318, respectively, and T and W product ions at *m/z* 304 and 233, respectively, as observed before for the minor WT GlcCer component. A minor $[M+Li]^+$ was also observed in the $^+$ESI-Q-TOF-MS profile of the MUT16 GlcCer at *m/z* 720 (Fig. 3B), decremented 14 u with respect to the major component; the CID product ion spectrum of this $[M+Li]^+$ (Fig. 5B) exhibited corresponding 14 u decrements to the O and N ions, now observed at *m/z* 466 and 304, respectively (the latter isobaric to the h16:0 T ion).

The $^+$ESI-MS data for the MUT24 strain GlcCer (data not shown) were essentially identical to those described above for the MUT16 component, and together they supported the somewhat surprising conclusion that the underlying mutation(s) has in each case resulted not only in ablation of the (*E*)-Δ^3-unsaturation of the fatty-*N*-acyl moiety but also in a virtually 100% shift in the dominant fatty-*N*-acyl chain length, shorter than that found in the WT GlcCer by two CH_2 units.

NMR spectroscopic analysis of *N. crassa* sterol glycosides

The one-dimensional ^{1}H-NMR spectrum of the putative sterol glycoside component isolated from *N. crassa* MUT24 is shown in **Fig. 6**. As with the GlcCer spectra analyzed above, a seven proton β-glucopyranosyl spin system is recognizable from the same characteristic set of resonances observed with similar chemical shifts and coupling patterns (resonances marked H-1′ to H-6a′ and H-6b′). The remaining resonances and their connectivities were assigned (see supplementary table) by acquisition and analysis of two-dimensional ^{1}H-^{1}H-gradient-enhanced correlation and -total correlation spectra (data not shown) along with a ^{1}H-detected ^{13}C-^{1}H-gradient-enhanced heteronuclear single-quantum correlation spectrum (see supplementary figure). Based on this analysis, along with comparison with published NMR spectral data (28), the glycolipid was identified as ergosterol-β-glucoside (Scheme 2), which was previously identified as the major sterol glycoside component of *P. pastoris* (29) and of transgenic *S. cerevisiae* expressing a UDP-Glc:sterol β-D-glucosyltransferase (*UGT*) gene from *P. pastoris* (28). The NMR data are indeed comparable with those published for 3β-(2,3,4,6-tetra-*O*-acetyl-β-D-glucopyranosyloxy) ergosta-5,7,22*E*-triene (28), allowing for somewhat predictable chemical shift increments attributable to that group's analytical choice of per-*O*-acetylating the β-D-glucosyl moiety, as well as for smaller differences resulting from the use of a different solvent and acquisition temperature in that work. NMR spectra obtained on the corresponding components from MUT16 and WT *N. crassa* were essentially identical to those shown for the MUT24 component, although the amount isolated from the WT strain was sufficient only for the acquisition of a one-dimensional ^{1}H-NMR spectrum.

DISCUSSION

In this work, we isolated and characterized two neutral glycolipid components from *N. crassa* not previously identified in this species; more significantly, we detected changes in their expression patterns in mutant strains selected for resistance to a radish defensin, RsAFP2 (11). These consisted of *i*) structural changes to the fatty-*N*-acyl moiety of

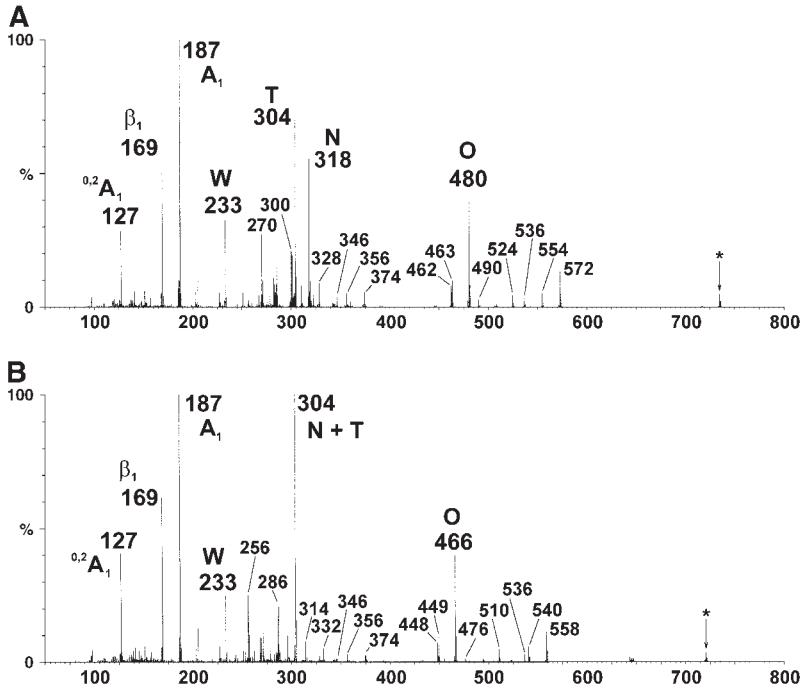

Fig. 5. Tandem $^+$ESI-MS/CID-MS product ion spectra of selected $[M+Li]^+$ from a *N. crassa* MUT16 GlcCer fraction. A: Product ion spectrum from *m/z* 734. B: Product ion spectrum from *m/z* 720.

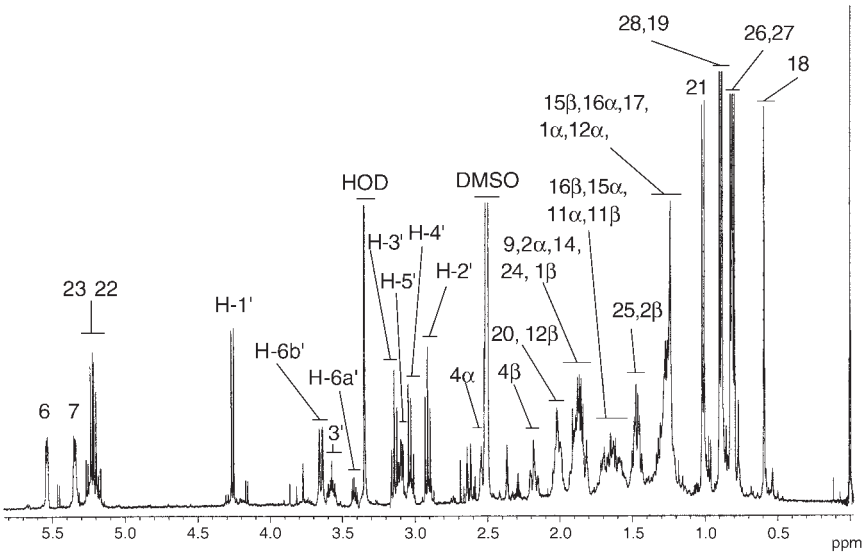

Fig. 6. One-dimensional ^{1}H-NMR spectrum of a GlcSte fraction isolated from *N. crassa* MUT24. Resonances from nonexchangeable protons of sterol (prefix omitted) and hexose (H) are designated by Arabic numerals, and those of the latter are primed. The corresponding structure and numbering are depicted in Scheme 2. HOD, residual monodeuterated water.

GlcCer found in both WT and mutant *N. crassa* strains [shortening of the dominant chain length from C18 to C16, and ablation of (*E*)-Δ^3-unsaturation], and *ii*) increased accumulation of GlcSte, identified as ergosterol-β-D-glucoside. Together with previously noted changes in the expression of acidic glycosphingolipids (11), which are still under investigation, it is apparent that the mutant strains exhibit a complex set of phenotypic alterations at the biochemical level. Whether these result from a single underlying mutation or from combinations of several mutations, and whether these mutations are actually in the genes coding for enzymes directly involved in the synthesis of the glycolipids in question, remain to be determined.

Previous studies have provided evidence that a variety of plant defensins interact with fungal sphingolipids as a primary step leading to growth arrest and that fungal GlcCer is a particular target of RsAFP2 (13). Moreover, selectivity with respect to ceramide structural features was displayed in ELISA-based binding assays, because RsAFP2 showed little interaction with GlcCer from plant or human sources, which lack one or more of the structural modifications found in fungal GlcCer (13). This suggests, on the one hand, that the observed changes in GlcCer structure between the WT and mutant *N. crassa* strains, such as the loss of fatty-*N*-acyl (*E*)-Δ^3-unsaturation, could have a direct effect on the binding interaction with RsAFP2. On the other hand, this hypothesis is not fully supported by the earlier biological assays of RsAFP2-GlcCer interactions, which were carried out using a *P. pastoris* system, or by the ELISA-based measurements of binding specificity, made with purified GlcCer from *P. pastoris* (13), because GlcCer from *P. pastoris* and other hemiascomycetous yeasts do not display the (*E*)-Δ^3-unsaturation under any circumstances. Thus, this feature is probably not essential for the interaction; therefore, it is unlikely that its ablation could by itself account for the loss of susceptibility to RsAFP2 displayed by the *N. crassa* mutants. Alternatively, it is possible that the shortening of the fatty-*N*-acyl chain in the mutant GlcCer could have an effect on its interaction with RsAFP2. There is evidence that such alterations in ceramide structure, even as

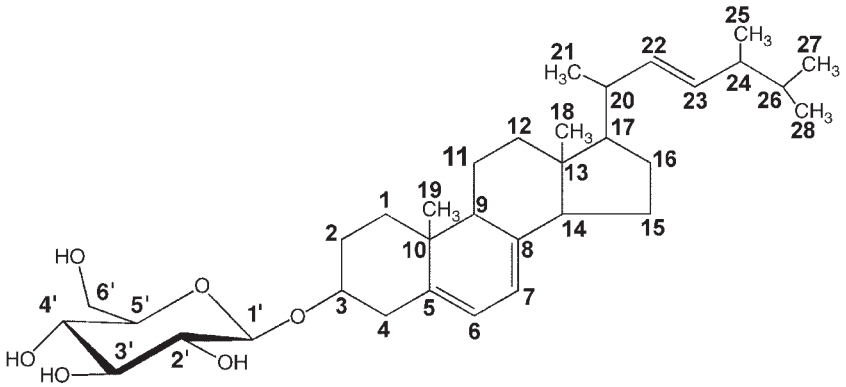

Scheme 3. Structure of ergosterol-β-D-glucopyranoside with numbering of sterol and hexose moieties.

subtle as a two carbon difference in fatty-*N*-acyl chain length, can modify the presentation of glycosphingolipids on the cell membrane surface, affecting their interactions with peptide and protein ligands (30, 31).

A third possibility is suggested by the increase in GlcSte levels observed in the mutant strains. There is evidence suggesting that fungal sterols could modulate the interaction of some defensins with their glycosphingolipid targets on the membrane surface, as addition of ergosterol was found to increase the interaction of another plant defensin, DmAMP1, with *S. cerevisiae* glycosylinositol phosphorylceramides in an ELISA (12). In addition, Ferket et al. (11) observed reduced sensitivity of the MUT16 and MUT24 mutants to the plant defensin HsAFP1; consistent with this, a *P. pastoris* mutant strain, *Δugt51*, lacking UGT activity, was found to be 4-fold more sensitive toward HsAFP1 (K. Thevissen, unpublished data). On the other hand, HsAFP1 does not appear to interact with sphingolipids, either GlcCer or glycosylinositol phosphorylceramides (K. Thevissen, unpublished data). Moreover, no significant change was observed in the sensitivity of the *P. pastoris Δugt51* mutant toward RsAFP2 (K. Thevissen, unpublished data). Although this does not completely rule out a relationship between increased GlcSte expression and decreased RsAFP2 sensitivity in the *N. crassa* mutants, considerably more work will be required to clarify whether it is a significant factor. It should be noted here that the apparent accumulation of GlcSte in the *N. crassa* mutants could also result from down-regulation of an as yet unknown β-glucosidase or other GlcSte-metabolizing enzyme.

In any case, GlcSte biosynthesis has been strongly implicated as a factor contributing to fungal phytopathogenicity and could be involved in the sensitivity of fungi to other plant defensins, as appears to be the case with HsAFP1. Functional characterization of *UGT* genes from a number of fungi, including *S. cerevisiae*, *C. albicans*, and *P. pastoris*, has been carried out by Warnecke et al. (28); they pointed out a highly similar sequence in a gene from *Magnaporthe grisea*, *pth8*, the disruption of which had previously been correlated with reduced pathogenicity (32). More recently, Kim et al. (33) also identified a putative factor in fungal disease virulence displaying strong homology to the *UGT* family through its deduced peptide sequence, the *chip6* gene from *Colletotrichum gloeosporioides* (*Glomerella cingulata* group), and demonstrated that its product expressed in *Escherichia coli* possessed UGT activity. Disruption of *chip6* in *C. gloeosporioides* resulted in an apparent reduction of UGT activity to 45% of the WT level and correlated with reduced pathogenicity toward its natural host, avocado fruit. In light of results described by Ferket et al. (11) and herein, it would be of interest to determine if the reduced pathogenicity of the *M. grisea* and *C. gloeosporioides ugt* mutants can be further correlated with increased binding and susceptibility to plant defensins such as RsAFP2 and HsAFP1.

Accumulation of GlcSte does not appear as widespread in the fungal kingdom as that of GlcCer (for recent discussions of the occurrence, biosynthesis, and possible functional roles of GlcCer in fungi, see 34, 35). Sakaki et al. (29) surveyed GlcSte and GlcCer expression in a number of fungi and found several that produced little or no detectable GlcSte under the culture conditions used; these included *C. albicans* and many strains of *P. pastoris*, both of which had been shown previously to have *UGT* genes (homologs of *S. cerevisiae UGT51*) encoding functional proteins (28). They also showed that GlcSte accumulates in one strain of *P. pastoris* in response to heat or ethanol shock, in contrast to GlcCer, which appears to be constitutively expressed. The evidence suggests that GlcSte is not essential for viability, although UGT51p-catalyzed biosynthesis of GlcSte was recently shown to be required for oxidative metabolism of small molecules, such as methanol or alkanes, by some fungi (36, 37).

Because the current study establishes that *N. crassa*, an established model fungal species, is capable of GlcSte biosynthesis, it may also prove to be a good system for studies of GlcSte function. As indicated by Sakaki et al. (29), tblastn (Basic Local Alignment Search Tool) queries (38) of the *N. crassa* genome databases (Munich Information Center for Protein Sequences, http://mips.gsf.de/proj/neurospora; and Whitehead Institute, http://www.broad.mit.edu/annotation/fungi/neurospora) (39) show that it contains three candidate genes encoding peptide sequences with a high degree of similarity to those of known fungal and plant *UGT* genes (MIPS codes xnc115_090, 3nc440_840, and 1nc130_180; Whitehead codes NCU09301.1, NCU00281.1, and NCU07473.1, respectively). The closest match for xnc115_090/NCU09301.1 appeared to be the putative *M. grisea pth8 UGT* (29). Kim et al. (33) pointed out the similarity between *chip6* and 1nc130_180/NCU07473.1; the closest match for 3nc440_840/NCU00281.1 also appears to be *chip6*. Systematic disruption or silencing experiments should identify which are active in GlcSte biosynthesis in WT *N. crassa*. Using this information, it would be of interest to determine whether susceptibility to RsAFP2 can be restored by disruption of *UGT* expression in the mutant strains.

This work was supported in part by the New Hampshire Biological Research Infrastructure Network-Center for Structural Biology [National Institutes of Health (NIH) P20 RR-16459], by the NIH Resource Center for Biomedical Complex Carbohydrates (NIH P41 RR-05351), and by Grant G.0288.04 from the Fonds voor Wetenschappelijk Onderzoek-Vlaanderen. I.E.J.A.F. is a postdoctoral fellow of the Fonds voor Wetenschappelijk Onderzoek-Vlaanderen (IWT/OZM/030508).

REFERENCES

1. Thomma, B. P. H. J., B. P. A. Cammue, and K. Thevissen. 2002. Plant defensins. *Planta.* **216:** 193–202.
2. Broekaert, W. F., B. P. A. Cammue, M. F. C. De Bolle, K. Thevissen, G. W. De Samblanx, and R. W. Osborn. 1997. Antimicrobial peptides from plants. *Crit. Rev. Plant Sci.* **16:** 297–323.
3. Thevissen, K., K. K. Ferket, I. E. Francois, and B. P. Cammue. 2003. Interactions of antifungal plant defensins with fungal membrane components. *Peptides.* **24:** 1705–1712.
4. Hoffmann, J. A. 1995. Innate immunity of insects. *Curr. Opin. Immunol.* **7:** 4–10.

5. Ganz, T. 2003. Defensins: antimicrobial peptides of innate immunity. *Nat. Rev. Immunol.* **3:** 710–720.
6. Bulet, P., C. Hetru, J. L. Dimarcq, and D. Hoffmann. 1999. Antimicrobial peptides in insects. Structure and function. *Dev. Comp. Immunol.* **23:** 329–344.
7. Thevissen, K., A. Ghazi, G. W. De Samblanx, C. Brownlee, R. W. Osborn, and W. F. Broekaert. 1996. Fungal membrane responses induced by plant defensins and thionins. *J. Biol. Chem.* **271:** 15018–15025.
8. Thevissen, K., F. R. Terras, and W. F. Broekaert. 1999. Permeabilization of fungal membranes by plant defensins inhibits fungal growth. *Appl. Environ. Microbiol.* **65:** 5451–5458.
9. Thevissen, K., R. W. Osborn, D. P. Acland, and W. F. Broekaert. 1997. Specific, high affinity binding sites for an antifungal plant defensin on *Neurospora crassa* hyphae and microsomal membranes. *J. Biol. Chem.* **272:** 32176–32181.
10. Thevissen, K., R. W. Osborn, D. P. Acland, and W. F. Broekaert. 2000. Specific binding sites for an antifungal plant defensin from dahlia (*Dahlia merckii*) on fungal cells are required for antifungal activity. *Mol. Plant Microbe Interact.* **13:** 54–61.
11. Ferket, K. K. A., S. B. Levery, C. Park, B. P. A. Cammue, and K. Thevissen. 2003. Isolation and characterization of *Neurospora crassa* mutants resistant to antifungal plant defensins. *Fungal Genet. Biol.* **40:** 176–185.
12. Thevissen, K., I. E. Francois, J. Y. Takemoto, K. K. Ferket, E. M. Meert, and B. P. Cammue. 2003. DmAMP1, an antifungal plant defensin from dahlia (*Dahlia merckii*), interacts with sphingolipids from *Saccharomyces cerevisiae*. *FEMS Microbiol. Lett.* **226:** 169–173.
13. Thevissen, K., D. C. Warnecke, I. E. Francois, M. Leipelt, E. Heinz, C. Ott, U. Zahringer, B. P. Thomma, K. K. Ferket, and B. P. Cammue. 2004. Defensins from insects and plants interact with fungal glucosylceramides. *J. Biol. Chem.* **279:** 3900–3905.
14. Osborn, R. W., G. W. De Samblanx, K. Thevissen, I. Goderis, S. Torrekens, F. Van Leuven, S. Attenborough, S. B. Rees, and W. F. Broekaert. 1995. Isolation and characterisation of plant defensins from seeds of Asteraceae, Fabaceae, Hippocastanaceae and Saxifragaceae. *FEBS Lett.* **368:** 257–262.
15. Thevissen, K., B. P. Cammue, K. Lemaire, J. Winderickx, R. C. Dickson, R. L. Lester, K. K. Ferket, F. Van Even, A. H. Parret, and W. F. Broekaert. 2000. A gene encoding a sphingolipid biosynthesis enzyme determines the sensitivity of *Saccharomyces cerevisiae* to an antifungal plant defensin from dahlia (*Dahlia merckii*). *Proc. Natl. Acad. Sci. USA.* **97:** 9531–9536.
16. Dickson, R. C., E. E. Nagiec, G. B. Wells, M. M. Nagiec, and R. L. Lester. 1997. Synthesis of mannose-(inositol-P)$_2$-ceramide, the major sphingolipid in *Saccharomyces cerevisiae*, requires the *IPT1* (*YDR072c*) gene. *J. Biol. Chem.* **272:** 29620–29625.
17. Terras, F. R., H. M. Schoofs, M. F. De Bolle, F. Van Leuven, S. B. Rees, J. Vanderleyden, B. P. Cammue, and W. F. Broekaert. 1992. Analysis of two novel classes of plant antifungal proteins from radish (*Raphanus sativus* L.) seeds. *J. Biol. Chem.* **267:** 15301–15309.
18. Leipelt, M., D. Warnecke, U. Zahringer, C. Ott, F. Muller, B. Hube, and E. Heinz. 2001. Glucosylceramide synthases, a gene family responsible for the biosynthesis of glucosphingolipids in animals, plants, and fungi. *J. Biol. Chem.* **276:** 33621–33629.
19. Toledo, M. S., E. Suzuki, A. H. Straus, and H. K. Takahashi. 1995. Glycolipids from *Paracoccidioides brasiliensis*. Isolation of a galactofuranose-containing glycolipid reactive with sera of patients with paracoccidioidomycosis. *J. Med. Vet. Mycol.* **33:** 247–251.
20. Toledo, M. S., S. B. Levery, A. H. Straus, E. Suzuki, M. Momany, J. Glushka, J. M. Moulton, and H. K. Takahashi. 1999. Characterization of sphingolipids from mycopathogens: factors correlating with expression of 2-hydroxy fatty acyl (*E*)-Δ^3-unsaturation in cerebrosides of *Paracoccidioides brasiliensis* and *Aspergillus fumigatus*. *Biochemistry.* **38:** 7294–7306.
21. Levery, S. B., M. Momany, R. Lindsey, M. S. Toledo, J. A. Shayman, M. Fuller, K. Brooks, R. L. Doong, A. H. Straus, and H. K. Takahashi. 2002. Disruption of the glucosylceramide biosynthesis pathway in *Aspergillus nidulans* and *Aspergillus fumigatus* by inhibitors of UDP-Glc:ceramide glucosyltransferase strongly affects spore germination, cell cycle, and hyphal growth. *FEBS Lett.* **525:** 59–64.
22. Dabrowski, J., P. Hanfland, and H. Egge. 1980. Structural analysis of glycosphingolipids by high-resolution ^{1}H nuclear magnetic resonance spectroscopy. *Biochemistry.* **19:** 5652–5658.
23. Yamada, A., J. Dabrowski, P. Hanfland, and H. Egge. 1980. Preliminary results of *J*-resolved, two-dimensional ^{1}H-NMR studies on glycosphingolipids. *Biochim. Biophys. Acta.* **618:** 473–479.
24. Dabrowski, J., H. Egge, and P. Hanfland. 1980. High resolution nuclear magnetic resonance spectroscopy of glycosphingolipids. I. 360 MHz ^{1}H and 90.5 MHz ^{13}C NMR analysis of galactosylceramides. *Chem. Phys. Lipids.* **26:** 187–196.
25. Levery, S. B., M. S. Toledo, R. L. Doong, A. H. Straus, and H. K. Takahashi. 2000. Comparative analysis of ceramide structural modification found in fungal cerebrosides by electrospray tandem mass spectrometry with low energy collision-induced dissociation of Li^+ adduct ions. *Rapid Commun. Mass Spectrom.* **14:** 551–563.
26. Toledo, M. S., S. B. Levery, E. Suzuki, A. H. Straus, and H. K. Takahashi. 2001. Characterization of cerebrosides from the thermally dimorphic mycopathogen *Histoplasma capsulatum*: expression of 2-hydroxy fatty *N*-acyl (*E*)-Δ^3-unsaturation correlates with the yeast-mycelium phase transition. *Glycobiology.* **11:** 113–124.
27. Hsu, F-F., and J. Turk. 2001. Structural determination of glycosphingolipids as lithiated adducts by electrospray ionization mass spectrometry using low-energy collisional-activated dissociation on a triple stage quadrupole instrument. *J. Am. Soc. Mass Spectrom.* **12:** 61–79.
28. Warnecke, D., R. Erdmann, A. Fahl, B. Hube, F. Muller, T. Zank, U. Zahringer, and E. Heinz. 1999. Cloning and functional expression of UGT genes encoding sterol glucosyltransferases from *Saccharomyces cerevisiae*, *Candida albicans*, *Pichia pastoris*, and *Dictyostelium discoideum*. *J. Biol. Chem.* **274:** 13048–13059.
29. Sakaki, T., U. Zahringer, D. C. Warnecke, A. Fahl, W. Knogge, and E. Heinz. 2001. Sterol glycosides and cerebrosides accumulate in *Pichia pastoris*, *Rhynchosporium secalis* and other fungi under normal conditions or under heat shock and ethanol stress. *Yeast.* **18:** 679–695.
30. Kiarash, A., B. Boyd, and C. A. Lingwood. 1994. Glycosphingolipid receptor function is modified by fatty acid content. Verotoxin 1 and verotoxin 2c preferentially recognize different globotriaosyl ceramide fatty acid homologues. *J. Biol. Chem.* **269:** 11138–11146.
31. Lingwood, C. A. 1996. Aglycone modulation of glycolipid receptor function. *Glycoconj. J.* **13:** 495–503.
32. Sweigard, J. A., A. M. Carroll, L. Farrall, F. G. Chumley, and B. Valent. 1998. *Magnaporthe grisea* pathogenicity genes obtained through insertional mutagenesis. *Mol. Plant Microbe Interact.* **11:** 404–412.
33. Kim, Y. K., Y. Wang, Z. M. Liu, and P. E. Kolattukudy. 2002. Identification of a hard surface contact-induced gene in *Colletotrichum gloeosporioides* conidia as a sterol glycosyl transferase, a novel fungal virulence factor. *Plant J.* **30:** 177–187.
34. Warnecke, D., and E. Heinz. 2003. Recently discovered functions of glucosylceramides in plants and fungi. *Cell. Mol. Life Sci.* **60:** 919–941.
35. Barreto-Bergter, E., M. R. Pinto, and M. L. Rodrigues. 2004. Structure and biological functions of fungal cerebrosides. *An. Acad. Bras. Cienc.* **76:** 67–84.
36. Stasyk, O. V., T. Y. Nazarko, O. G. Stasyk, O. S. Krasovska, D. Warnecke, J. M. Nicaud, J. M. Cregg, and A. A. Sibirny. 2003. Sterol glucosyltransferases have different functional roles in *Pichia pastoris* and *Yarrowia lipolytica*. *Cell Biol. Int.* **27:** 947–952.
37. Oku, M., D. Warnecke, T. Noda, F. Muller, E. Heinz, H. Mukaiyama, N. Kato, and Y. Sakai. 2003. Peroxisome degradation requires catalytically active sterol glucosyltransferase with a GRAM domain. *EMBO J.* **22:** 3231–3241.
38. Altschul, S. F., W. Gish, W. Miller, E. W. Myers, and D. J. Lipman. 1990. Basic local alignment search tool. *J. Mol. Biol.* **215:** 403–410.
39. Galagan, J. E., S. E. Calvo, K. A. Borkovich, E. U. Selker, N. D. Read, D. Jaffe, W. FitzHugh, L.-J. Ma, S. Smirnov, S. Purcell et al. 2003. The genome sequence of the filamentous fungus *Neurospora crassa*. *Nature* **422:** 859–868.
40. Domon, B., and C. E. Costello. 1988. Structure elucidation of glycosphingolipids and gangliosides using high-performance tandem mass spectrometry. *Biochemistry.* **27:** 1534–1543.
41. Domon, B., J. E. Vath, and C. E. Costello. 1990. Analysis of derivatized ceramides and neutral glycosphingolipids by high-performance tandem mass spectrometry. *Anal. Biochem.* **184:** 151–164.
42. Costello, C. E., and J. E. Vath. 1990. Tandem mass spectrometry of glycolipids. *Methods Enzymol.* **193:** 738–768.
43. Adams, J., and Q. Ann. 1993. Structure determination of sphingolipids by mass spectrometry. *Mass Spectrom. Rev.* **12:** 51–85.